Journal Article

Crack growth in a naturally corroded bridge steel

Ali, K., Peng, D., Jones, R., Singh, R. R. K., Zhao, X. L., McMillan, A.J. and Berto, F

CRACK GROWTH IN A NATURALLY CORRODED BRIDGE STEEL

K. Ali[1], D. Peng[1], R. Jones[1], R. R. K. Singh[1], X. L. Zhao[2], A. J. McMillan[3], F. Berto[4]

[1]Department of Mechanical and Aerospace Engineering, Monash University, Clayton, Vic 3800, Australia.

[2]Department of Civil Engineering, Monash University, Clayton, Vic 3800, Australia.

[3]Division of Applied Science, Computing and Engineering, Glyndwr University, Wrexham, LL11 2AW, Wales, UK.

[4] Norwegian University of Science and Technology - NTNU, Department of Engineering Design and Materials, Trondheim, 7491, Norway

SUMMARY

This paper summarises the findings of an international collaborative program that focuses on the problem of the growth of cracks that arise from natural corrosion in bridge steels. The experimental data presented in this paper confirms that the bridge steel da/dN versus ΔK relationship is similar to that seen by the high strength aerospace steels D6ac and 4340. It is then shown that the methodology developed to predict the growth of small naturally occurring cracks in aerospace materials can also be used to compute the growth of cracks that arise due to natural corrosion in bridge steels.

Keywords: Aging bridges; corrosion, fatigue crack growth; ASTM E647-13a; aerospace steels

NOMENCLATURE

a	crack length
A	a constant in the Hartman-Schijve variant of the NASGRO crack-growth equation
da/dN	rate of crack growth per cycle
D	a constant in the Hartman-Schijve crack-growth equation
K	stress-intensity factor
K_{max}	maximum value of the applied stress-intensity factor in the fatigue cycle
K_{min}	minimum value of the applied stress-intensity factor in the fatigue cycle
ΔK	range of the applied stress-intensity factor in the fatigue cycle, as defined below
ΔK	$= K_{max} - K_{min}$
ΔK_{th}	the fatigue threshold value of the applied stress-intensity factor, as defined in ASTM E647-13a
ΔK_{thr}	the apparent fatigue threshold value of the applied stress-intensity factorused in the Hartman-Schijve crack-growth equation
m	exponent in the Hartman-Schijve crack-growth equation
N	number of fatigue cycles
R	stress ratio ($= \sigma_{min}/\sigma_{max}$)
R^2	the linear correlation coefficient
ACR	Adjusted compliance ratio

1. INTRODUCTION

The 2013 report [1] into safety of US bridges found that one in nine were rated as being "structurally deficient" and that this was largely due to the cumulative effect of corrosion. In this context the US Federal Highway Administration Steel Bridge Design Handbook [2] states:

a) "..there is little or no time during the life of the structure that is taken up with "initiating" cracks."

b) "As much as 80% of the fatigue life has been consumed by the time a fatigue crack emanating from an internal flaw reaches the surface and can be observed."

Thus in this study attention is focused on the use of fracture mechanics[1] and fatigue crack growth[2] approaches to compute the growth of cracks from natural corrosion in a bridge steel In this context it should be noted that it is now well known [8-10] that the effect of corrosion on structural integrity is exacerbated by the topography of the surface corrosion which results in localised stress concentrators which in turn accelerate both the initiation and the growth of cracks.

The conclusions, i.e. points a) and b) above, mirror those associated with crack growth in operational aircraft where it has long been known [7, 11-15] that the operational life of aircraft is governed by the growth of lead cracks, i.e. the fastest cracks in the structure. Lead cracks in aircraft exhibit the following features, viz:

i. They start to grow shortly after the aircraft is introduced into service.
ii. The majority of the life is consumed growing to a size that can be detected using existing non destructive inspection techniques.

As previously mentioned this behaviour mirrors the findings reported in [2].

The similarity between cracking in bridges and aircraft is further reinforced by the findings reported in [16] which presented pictures of the cracking in a bridge section [17] together with pictures of cracking in the D6ac steel wing pivot fitting in the 1969 General Dynamics, now Lockheed, F-111 wing fatigue test[3], see Figures 1 and 2 respectively. These figures show how in each case cracking grew from small sub mm material discontinuities.

This observation led [16] to establish that the da/dN versus ΔK relationship proposed by the Japan Society of Steel Construction (JSSC) [18] and by Barsom and Rolfe [6] for bridge steels essentially coincided with that of the high strength aerospace steel D6ac given in [20]. In this paper we build on this observation by comparing the da/dN versus ΔK data associated with a range of the growth of cracks associated with a range of bridge steels with the

[1] References [2-6] provide excellent summaries of the state of the art in the use of fracture mechanics based tools fatigue assessment of bridges and bridge steels.
[2] A review of recent advances in fatigue assessment is given in [7].
[3]The in-flight failure of a USAF F-111 led to the development of the damage tolerance design philosophy [27].

equations given in [6] and [19] as well as with the corresponding data given in [20] for the high strength aerospace steel 4340. We then show that the bridge steel da/dN versus ΔK relationship can be described by the Hartman-Schijve variant [7] of the Nasgro equation [21].

Since, as discussed above, the growth of cracks in aging bridges is often associated with small sub mm cracks and since the fatigue standard ASTM E647-13a [22] suggests that the da/dN versus ΔK relationship associated with the growth of such small cracks can be approximately determined from tests on long cracks and correcting for closure effects we then shown how the short crack da/dN versus ΔK curve obtained for 4340 steel [23] is also captured as outlined in [7] by setting the threshold term in the Nasgro representation (for bridge steels) to a small value. To build on this observation we next show how the da/dN versus ΔK curve obtained for the growth of small sub mm cracks in a 350 MPa grade mild steel follows the same Nasgro representation albeit with the threshold term set to a slightly smaller value.

These results suggest that the initiation and growth of cracks from natural corrosion in a bridge steel should also conform to the Nasgro equation[4] with the constants determined in the previous long crack studies the threshold term set to a small value. This hypothesis is subsequently confirmed experimentally. As such the present paper suggests that not only is the da/dN versus ΔK curve for bridge steels similar to that seen for the high strength aerospace steels D6ac and 4340 but the methodology developed to assess the growth of small sub mm cracks in aerospace materials [7, 24-26] is also applicable to cracks that initiate and grow from natural corrosion in a bridge steel.

2. CRACK GROWTH IN BRIDGE STEELS

The United States Air Force has concluded that the most appropriate way to address the problem of aging structures is via the discipline of fracture mechanics [27, 28]. This approach has also been widely used to assess fatigue cracking in bridge steels [3, 6, 4]. In this context [16] has established that the da/dN versus ΔK relationship proposed by the Japan Society of Steel Construction (JSSC) [18] and by Barsom and Rolfe [6] for bridge steels essentially coincided with that of the high strength aerospace steel D6ac given in [20].

To further examine this conclusion, i.e. that fatigue crack growth in bridge steels is essentially independent of the type of steel and that the associated da/dN versus ΔK relationship is similar to that seen in high strength aerospace steels, we considered crack growth in five different bridge steels which were tested at a range of R ratio's, viz:

i) A36, where the crack growth data was taken from [6, 29], which is common in older bridges.

ii) HPS 485W a high performance bridge steel used in North American bridges [19].

[4] Here it should be noted that with the exception of the crack growth analysis presented in [9], which used a fractal based crack growth equation, most approaches to this class of problems are based upon the use of S/N curves [8] to determine the life to crack initiation. A feature of the present study is that it suggests that commercially available crack growth computer programs can be used to determine the total life of corroded components.

iii) HPS 350WT a high performance bridge steel with an improved low temperature performance [30].

iv) A588-80A [30], a weathering steel that is widely used in bridges. This steel has little R ratio dependency, see [31].

v) The Chinese bridge steel 14MnNbq [32].

The da/dN versus ΔK curves for these five bridge steels are shown in Figure 3, along with the da/dN versus ΔK relationship suggested by the Japan Society of Steel Construction (JSSC) [18], viz:

$$da/dN = 1.5 \times 10^{-11} (\Delta K)^{2.75} \quad (1)$$

Figure 3 also presents the da/dN versus ΔK relationship suggested in [6], viz:

$$da/dN = 6.86 \times 10^{-12} (\Delta K)^{3} \quad (2)$$

and the da/dN versus ΔK relationship suggested by Fisher et al in [19]

$$da/dN = 1.0 \times 10^{-11} (\Delta K)^{3} \quad (3)$$

to describe an upper bound on crack growth in bridge steels.

Here we see that, allowing for experimental error, the crack growth behaviour of these various steels is indeed very similar and, as such, extends the conclusion reached by the US Federal Highway Administration [17], which was based on examining the S-N curves for a (different) range of bridge steels to cover crack growth in bridge steels. Figure 3 also reveals that the ASTM E647-13a long crack da/dN versus ΔK curve can be approximated by the curve BCD, which represents an average of the various da/dN versus ΔK curves. The values of da/dN and ΔK that define the curve BCD are given in Table 1.

Another outcome of this study is that, as per the crack growth behaviour of D6ac steel [33], allowing for experimental error the bridge steels experimental da/dN versus ΔK curves appears to show little, if any R, ratio effect. This conclusion is also implicit in the Japan Society of Steel Construction (JSSC) [18], the Barsom and Rolfe [6] and the Fisher et al in [19] recommended da/dN versus ΔK relationships, i.e. equations (1)-(3), since these equations have no R ratio dependency. The absence of a significant R ratio effect for these long crack tests means that long cracks in bridge steels will exhibit little, if any, plastic wake induced crack (tip) closure [7, 33, 34].

To continue this study Figure 4 presents a comparison of the bridge steel curve BCD with the NASA experimental da/dN versus ΔK curves for 4340 steel [20] which as can be seen in Figure 4 are essentially R ratio independent. Noting that, as shown in [7], the growth of both long and short cracks in D6ac could be expressed as per the Hartman-Schijve variant of the Nasgro equation, viz:

$$da/dN = D\,[(\Delta K - \Delta K_{thr})/\sqrt{(1-K_{max}/A)}]^m \qquad (4)$$

with $D = 2.0 \times 10^{-10}$ and m = 2 and that the crack growth behaviours of D6ac and 4340 steels are similar Figure 4 also illustrates how the growth of cracks in 4340 steel can be captured using equation (4) with the values $D = 2.0 \times 10^{-10}$ and m = 2 together with the value of A given in [35] for 4340 steel, i.e. A = 160 MPa √m, and a threshold value of ΔK curves= 6.5 MPa √m. As a result we see that not only is the da/dN versus ΔK curve for bridge steels similar to that seen by D6ac steel [16] it is also similar to the da/dN versus ΔK curve associated with the high strength aerospace steel 4340. As such it suggests that crack growth in bridge steels should be able to be captured by the Hartman-Schijve variant of the Nasgro equation, i.e. equation (4), albeit with slightly different constants.

3. THE NASGRO REPRESENTATION OF CRACK GROWTH IN BRIDGE STEELS

Given the da/dN versus ΔK data shown in Figure 3 the associated NASGRO equation[5] for bridge steels can now be determined. This can be done as outlined in [7, 35] by plotting da/dN versus the term $((\Delta K - \Delta K_{thr})/\sqrt{(1-K_{max}/A)})$, see Figure 5. From Figure 5 it can be seen that crack growth in each of these different steels can be expressed as per the NASGRO equation[6]:

$$da/dN = 1.5 \times 10^{-10}\,((\Delta K - \Delta K_{thr})/\sqrt{(1-K_{max}/A)})^2 \qquad (5)$$

where ΔK_{thr} is a threshold term and A is the cyclic fracture toughness, see [7, 25] for a more detailed explanation of this form of the NASGRO equation. The values of ΔK_{thr} and A associated with these steels are given in Table 2 and an explanation of how these values were obtained is given in the Appendix. Here it should be noted that, as expected since crack growth in bridge steels is similar to that in D6ac and 4340 steels, the constant of proportionality in equation (5), i.e. $D = 1.5 \times 10^{-10}$, is similar to the value of D for these two high strength aerospace steel (i.e. $D = 2.0 \times 10^{-10}$).

---

[5] The NASGRO crack growth equation is available in most commercially available crack growth computer programs.

[6] The NASGRO equation is discussed in more detail in [7, 21].

4. NASGRO REPRESENTATION OF SHORT CRACK GROWTH IN 4340 STEEL

The fatigue test standard ASTM E647-13a [22] explains that the fatigue threshold associated with cracks that initiate and grow from small naturally occurring material discontinuities is generally small, i.e. much smaller than the corresponding large crack threshold. Furthermore, for small cracks in operational structure the very existence of a fatigue threshold is questioned in [22]. Hence, as first shown in [36] and discussed in more detail in [7, 24-26, 37], the behaviour of cracks that arise and grow naturally[7] can often be approximated by a Paris like crack growth equation. For mild steels this observation was first shown in [38] for BS4360-43A. In this study it was shown that the growth of short (approximately 0.2 mm initial cracks) could be described by the Hartman Schijve equation:

$$da/dN = 1.14 \times 10^{-10} ((\Delta K - \Delta K_{thr})^{1.95} \qquad (6)$$

Comparing equation (6) with equation (5) we see that the two equations are very similar. Subsequent studies have built on this finding, i.e. on [38], to the extent that it is now known that the growth of cracks from small naturally occurring material discontinuities can be approximated by the Hartman-Schijve variant of the Nasgro equation long crack, i.e. equation (4), with the constants D and A obtained from tests on long cracks using a reduced value of the threshold term ΔK_{thr} [7, 24-26, 39]. Indeed, as explained in [7, 24, 25] for a given size crack the scatter in the da/dN versus ΔK curves can often be captured by allowing for small changes in the term ΔK_{thr}. To illustrate this [7] considered the paper by Virkler, Hillberry and Goel [40] which is recognised as being one of the definitive studies that illustrates the variability in crack growth rates. The paper Virkler, Hillberry and Goel presented the results of sixty eight R = 0.2 tests on 2024-T3 panels where the initial crack length was 9 mm. In Jones [7] it was shown that this variability is captured reasonably well by merely allowing for small changes in ΔK_{thr}, i.e. using vales of 2.9, 3.2, 3.4, 3.6, 3.8, 4 and 4.2. Whilst the variability in crack growth is greater for small cracks than for long cracks it has also been shown [7, 24-26] that the associated variability is also captured by allowing for small changes in ΔK_{thr}. Thus as explained in [7, 24-26] for a given crack size the threshold term is not unique and that there is a family of da/dN versus ΔK curves.

In this context it is now also thought [7, 22, 41, 42] that the da/dN versus ΔK relationship associated with short cracks can often be approximated by the "closure corrected" long crack curve. Consequently noting the similarity in the da/dN versus ΔK curves associated with cracking in bridge steels and cracking in 4340 and that, as will be shown later, crack growth in corroded bridge steels is often associated with small sub mm initial cracks Figure 6 also presents the "closure free" curve for 4340 steel measured in [23] using a variant[8] of the ASTM E647-13a compliance offset method which is outlined in Appendix X2 of ASTM E647-13a. In Figure 6 this "short crack" curve is labelled the R = 0.4 OP1 curve. Furthermore, noting that, as suggested in [24], the short crack da/dN versus ΔK curve can often be represented as per equation (4) by using a lower value of the threshold term ΔK_{thr} than that associated with the corresponding long crack curve Figure 6 also presents the

[7] From small naturally occurring material discontinuities.

[8] Whereas Appendix X2 recommends a 2% offset [23] used a 1% offset and as such the data presented in can be expected to slightly underestimate crack growth.

computed "closure free" da/dN versus ΔK curve obtained using equation (5) with a threshold term ΔK_{thr} of 4 MPa √m. As such Figure 6 supports the conclusion, stated in [24] that, allowing for experimental error, if a reduced threshold term is used then the resultant computed and the OP1 estimated "short crack" curves are in good agreement.

5. NASGRO REPRESENTATION OF SHORT CRACK GROWTH IN A MILD STEEL

Having seen that the Nasgro equation can be used to represent the growth of both long and short cracks in 4340, that despite the differences in yield stress and hardness the growth of cracks in bridge steels and high strength aerospace steels is similar and that the Hartman-Schijve equation was able to capture the growth of short cracks in BS4360-43A steel let us next address its ability to capture the growth of small cracks in a 350 grade mild steel. To this end consider the crack growth data presented in [43] for a 350 grade mild steel specimens cut from a freight wagon. In these tests the crack was allowed to arise naturally from a 1 mm radius semicircular edge notch. The specimens were tested at a range of R ratio's. The initial crack lengths varied from approximately 0.1 mm to 1 mm. The test envelope is shown in Table 3 and the associated da/dN versus ΔK curves are given in Figure 7 which also contains the da/dN versus ΔK relationship corresponding to equation (4) with the values $D = 2.0 \times 10^{-10}$ and m = 2, A = 140 MPa √m and ΔK_{thr} = 0.1 MPa √m:

$$da/dN = 2 \times 10^{-10} ((\Delta K - \Delta K_{thr})/\sqrt{(1-K_{max}/140)})^2 \qquad (7)$$

This value of ΔK_{thr} is similar to that seen for small lead cracks in 7050-T7451 and 7075-T6 [24]. Indeed, Figure 7 reveals that equation (7) is a reasonably good approximation to the growth of small cracks in this steel.

Figure 7 also reveals that, allowing for experimental error, the growth of these small cracks in this steel is similar to the growth of small cracks in aerospace materials in that the associated da/dN versus ΔK curves exhibit little R ratio dependency and have a near Paris like shape with a low fatigue threshold.

6. TESTING AND ANALYSIS OF CORRODED BRIDGE STEELS

The previous sections have established that the bridge steels da/dN versus ΔK curves are similar to those of the two high strength aerospace steels D6ac and 4340; that the Hartman-Schijve equation is a reasonably good representation for the growth of long cracks in bridge steels; that as explained in [7] the growth of small cracks in 43340 and a 350 MPa grade mild steel can be approximated by the Hartman-Schijve variant of the Nasgro equation long crack, i.e. equation (4), with the constants D and A obtained from tests on long cracks using a reduced value of the threshold term ΔK_{thr}.

The question thus arises: Can this approach, i.e. use of the Hartman-Schijve variant of the Nasgro equation long crack with the constants D and A obtained from tests on long cracks using a reduced value of the threshold term ΔK_{th}, be used to compute the growth of cracks that arise and grow in bridge steels as a result of naturally corrosion**?**

To answer this question we cut a specimen from a badly corroded steel bridge section that was taken from sections of a condemned bridge provided by V/Line, see Figure 8. This specimen was fatigued under a repeated marker load block spectrum with a peak stress of 300 MPa. Each load block consisted of 1000 cycles at R = 0.1 and 7000 cycles at R = 0.5. The marker block loading was designed to allow the crack growth history to be obtained via quantitative fractography.

To assist in loading the specimen the corrosion in the area to be gripped was removed. This meant that there was a small (approximately) 1 mm increase[9] in section thickness immediately outside of the grips, see Figures 8 and 9. This was expected to introduce a small bending stress in the working section. As a result it was necessary to determine the stress distribution and the stress intensity factor solutions using finite element analysis[10]. Symmetry considerations meant that only ½ of the specimen needed to be modelled, see Figure 9.

As explained in [8-10] the topography of the corroded surface can play a significant role in both crack initiation and growth. (Pictures of the corroded surface are presented in Figures 10 and 11.) Thus after testing the corrosion products were removed using a steel brush and the surface profile was measured. This profile was then used in the finite element model. In this analysis the corrosion products were not modelled. The resultant stress distribution, for a load of 204 kN, is shown in Figure 12.

The next stage of this study was to use the stress field determined from the finite element model shown in Figure 12 to compute crack growth seen in this test and to compare the predictions with the experimental measurements. This crack growth analysis used the Nasgro representation of the da/dN versus ΔK curve for bridge steels given in equation (5). As in [7, 24-25] to capture the scatter in the crack growth histories associated with the various cracks small changes in the threshold term ΔK_{thr} were allowed. The thresholds used in these analyses are given in Table 4.

The experimental test produced a number of cracks, see Figure 13 where we see three dominant cracks. The sizes of the initiating features associated with these cracks were determined from SEM, see Figure 14, and estimates are given in Table 4. These sizes were used as the initial crack sizes in the fatigue analyses. The resultant computed, using equation (5) with the threshold[11] terms as given in Table 4, and measured crack growth histories are shown in Figure 15 where we see excellent agreement. Here it should be noted that there is a discontinuity in the slope of the crack depth versus load blocks curve when the crack transitions to a through-the-thickness crack. It should also be noted that in this analysis the threshold values varied from approximately 0.5 to 1.9 MPa $\sqrt{m}$. This variation is consistent with that reported in [24] for the growth of cracks from etch pits.

[9] This does not include the height of the corroded material.
[10] The stress intensity factors were determined, as recommended in [7], using the stress field in conjunction with three dimensional weight function theory.
[11] These thresholds were determined by matching the initial slopes of the crack depth versus load block curve.

7. CONCLUSION

This paper has outlined a building block approach that illustrates the ability to estimate the effect of natural corrosion on the structural integrity of aging steel bridges. To this end it is first shown that the bridge steel da/dN versus ΔK relationship is similar to that seen by the high strength aerospace steels D6ac and 4340. The Hartman-Schijve representation of the growth of long cracks in bridge steels is then determined. It is then shown that the methodology developed to predict the growth of small naturally occurring cracks in aerospace materials, i.e. by using the Hartman-Schijve variant of the Nasgro equation with the constants D and A obtained from tests on long cracks together with a reduced value of the threshold term ΔK_{thr}, can also be used to compute the growth of cracks that arise due to natural corrosion in a bridge steel.

8. REFERENCES

1. Davis SL., DeGood K., Donohue N. and Goldberg D, (2013) The Fix We're In For: The State of Our Nation's Busiest Bridges, Transportation for America, http://t4america.org/docs/bridgereport2013/2013BridgeReport.pdf
2. Mertz D., Steel Bridge Design Handbook: Design for Fatigue, (2012) U.S. Department of Transportation, Federal Highway Administration, Publication No. FHWA-IF-12-052 - Vol. 12, November 2012.
3. Fisher JW., Fatigue Design: Its past, what it is today and its future, http://mceer.buffalo.edu/education/bridge_speaker_series/2010-2011/flyers/Fisher_flyer.pdf
4. Fisher JW., Kulak GL., Smith AFC., (1988) A Fatigue Primer for Structural Engineers, Published by National Steel Bridge Alliance, May 1988. Available at https://www.aisc.org/store/p-1638-a-fatigue-primer-for-structural-engineers-pdf-download.aspx
5. Fisher JW., Nussbaumer A., Keating PB., Yen BT., (1993) Resistance of Welded Details Under Variable Amplitude Long-Life Fatigue Loading, National Cooperative Highway Research Program, NCHRP Report 354, ISBN 0-309-05352-8.
6. Barsom, J. M., and Rolfe, S. T. (1999) Fracture and fatigue control in structures: Applications of fracture mechanics, 3rd Ed., ASTM MNL41, ASTM, West Conshohocken, PA.
7. Jones R., Fatigue Crack Growth and Damage Tolerance, (2014) Fatigue and Fracture of Engineering Materials and Structures, 37, 5, pp. 463–483. available on line at: http://onlinelibrary.wiley.com/journal/10.1111/(ISSN)1460-2695/homepage/virtual_issue__fatigue_and_fracture_of_aerostructures.htm
8. Rusk DT., Hoppe W., Braisted W., Powar N., (2009) Fatigue life prediction of corrosion-damaged high-strength steel using an equivalent stress riser (ESR) model. Part II: Model development and results, Int. J. Fatigue, 31, pp. 1454-1463.
9. Shan-hua Xu, Bin Qiu, (2013) Experimental study on fatigue behavior of corroded steel, Materials Science & Engineering A, 584, pp.163–169.
10. Nakamura S., Suzumura K., (2013) Experimental Study on Fatigue Strength of Corroded Bridge Wires, J. Bridge Eng., 18, 3, pp. 200-209.
11. Berens AP., Hovey PW., Skinn DA., (1991) Risk analysis for aging aircraft fleets - Volume 1: Analysis, WL-TR-91-3066, Flight Dynamics Directorate, Wright Laboratory, Air Force Systems Command, Wright-Patterson Air Force Base, October 1991.

12. Barter SA., Molent L., Wanhill RH., (2012) The lead crack lifing framework, International Journal of Fatigue, 41, pp. 1-198.
13. Rudd JL., Yang JN., Manning SD. and Yee BW. (1982) Probabilistic fracture mechanics analysis methods for structural durability, Proceedings of the Meeting of the AGARD Structures and Materials Panel (55th), Toronto, Canada, 19-24 available at http://handle.dtic.mil/100.2/ADP001608.
14. Yang YN. and Hsi WH. and Manning SD., (1985) Stochastic crack propagation with applications to durability and damage tolerance analyses, AFWAL-TR-85-3062, Flight Dynamics Directorate, Wright Laboratory, Air Force Systems Command, Wright-Patterson Air Force Base, September 1985.
15. Manning SD. and Yang YN., (1987) Advanced durability analysis Volume I-Analytical methods, AFWAL-TR-86-3017, Flight Dynamics Directorate, Wright Laboratory, Air Force Systems Command, Wright-Patterson Air Force Base, July 1987.
16. Ali K., Singh RRK., Zhao XL., Jones R. and McMillan AJ., (2016) Composite repairs to bridge steels demystified, Journal of Composite Structures, http://dx.doi.org/10.1016/j.compstruct.2016.07.049.
17. Dexter RJ., and Ocel JM., (2013) Manual for Repair and Retrofit of Fatigue Cracks in Steel Bridges, US Department of Transportation, Federal Highway Administration Report FHWA-IF-13-020.
18. Japan Society of Steel Construction (JSSC), (1995) Fatigue design recommendations for steel structures.
19. Fisher JW., Nussbaumer A., Keating PB., Yen BT.,(1993) Resistance of Welded Details Under Variable Amplitude Long-Life Fatigue Loading, National Cooperative Highway Research Program, NCHRP Report 354, ISBN 0-309-05352-8.
20. Forth SC., James MA., Newman JA. Everett, RA. Jr., and Johnston WM. Jr., (2004) Mechanical data for use in damage tolerance analyses, NASA/TM-2004-213503 and ARL-TR-3375.
21. Forman, RG., and Mettu, SR. (1992) Behavior of Surface and Corner Cracks Subjected to Tensile and Bending Loads in Ti-6Al-4V Alloy, Fracture Mechanics 22nd Symposium, Vol. 1, ASTM STP 1131, H.A. Ernst, A. Saxena and D.L. McDowell, eds., American Society for Testing and Materials, Philadelphia, 1992.
22. ASTM. (2014) Measurement of fatigue crack growth rates. ASTM E647-13a, USA.
23. Yamada Y., Newman JC., (2010) Crack closure under high load ratio and K_{max} test conditions, Procedia Engineering, 2, pp. 71-82.
24. Jones R., Huang P. and Peng D., (2016) Crack growth from naturally occurring material discontinuities under constant amplitude and operational loads, International Journal of Fatigue, 91 pp. 434–444.
25. Molent L., Jones R (2016) The influence of cyclic stress intensity threshold on fatigue life scatter, International Journal of Fatigue, 82, pp. 748-756.
26. Jones R, Molent L and Barter S., (2013) Calculating crack growth from small discontinuities in 7050-T7451 under combat aircraft spectra, Int J. Fatigue, 55, pp. 178-182.
27. Tiffany CF., Gallagher JP., Babish IV CA. (2010) Threats to aircraft structural safety, including a compendium of selected structural accidents/incidents, Aeronautical Systems Center, Engineering Directorate, Wright-Patterson Air Force Base, ASC- TR-2010-5002.
28. Miedlar PC., Berens AP., Gunderson A., and Gallagher JP., Analysis and support initiative for structural technology (ASIST), AFRL-VA-WP-TR-2003-3002.

29. Fisher JW., Mertz DR. Zhong A., (1983) Steel bridge members under variable amplitude, long life fatigue loading, National Cooperative Highway Research Program, NCHRP Project 12-15(4), Report 267, Transportation Research Board.
30. Chen H., Grodin GY and Driver RG,. (2002) Fatigue Resistance of high performance steel, Sixth International Conference on Short & Medium Span Bridges, Vancouver, Canada, 31st July – 2nd August, 2002.
31. Zweraeman FJ. and Frank KH., (1988) Fatigue damage under variable amplitude loads, Journal of Structural Engineering, 114, 1, pp. 67-83.
32. Yan-Ping Liu, Chuan-Yao Chen and Guo-Qing, (2012) Fatigue crack growth and control of 14MnNbq welding plates used for bridges, ASCE Journal Of Engineering Mechanics, 138, pp. 30-35.
33. Forth SC., James MA., Johnston WM., and Newman JC. Jr., (2007) Anomalous Fatigue Crack Growth Phenomena In High-Strength Steel, Proceedings 11th International Congress on Fracture (ICF11), Italy, Available on line at http://www.gruppofrattura.it/ocs/index.php/ICF/ICF11/paper/view/10368/9732.
34. Ritchie RO., (1977) Near-Threshold Fatigue Crack Propagation in Ultra-High Strength Steel: Influence of Load Ratio and Cyclic Strength, Journal of Engineering Materials and Technology, pp. 195-204.
35. Jones R., Molent L., Walker K. (2012) Fatigue crack growth in a diverse range of materials, Int. J. Fatigue, 40, pp. 43-50.
36. Lincoln JW., Melliere RA. (1999) Economic Life Determination for a Military Aircraft, AIAA Journal of Aircraft, 36, 5. 737-742.
37. Jones R. and Tamboli D., (2013) Implications of the lead crack philosophy and the role of short cracks in combat aircraft, Engineering Failure Analysis, 29, pp.149-166.
38. Smith IFC., Smith RA., (1983) Fatigue crack growth in a fillet welded joint, Engineering Fracture Mechanics, 18, 4, pp. 861-869.
39. Tan JT. and Chen BK., (2015) Prediction of fatigue life in aluminium alloy (AA7050-T7451) structures in the presence of multiple artifical short cracks, Theoretical Applied Fracture Mechanics, 78, pp 1-7.
40. Virkler DA., Hillberry BM., Goel PK. (1979) The statistical nature of fatigue crack propagation, Trans ASME,101, pp.148–53.
41. Lados DA., Apelian D., Paris PC., Donald JK. (2005) Closure mechanisms in Al–Si–Mg cast alloys and long-crack to small-crack corrections, International Journal of Fatigue, 27, pp.1463–1472.
42. Park J. and Garcia W., (2015) Impacts on Crack Growth Analysis of Ti-6Al-4V Small Crack Test Data, 2015 Aircraft Structural Integrity Program (ASIP), The Hyatt Regency, San Antonio, Texas, USA; 1st-3rd December 2015.
43. Jones R, Pitt S., and Peng D., The Generalised Frost-Dugdale approach to modeling fatigue crack growth, Engineering Failure Analysis, Engineering Failure Analysis, 15, 8, 2008, pp 1130-1149.

APPENDIX

This section briefly describes how the constants in the Harman-Schijve variant of the Nasgro equation, i.e. equation (4), can be determined from the measured da/dN versus ΔK data. To this end, for a given R ratio, da/dN is plotted (in Excel) against $\left[\frac{\Delta K - \Delta K_{thr}}{\sqrt{\{1 - K_{max}/A\}}}\right]$ using log-log scales. Here the value of A is initially chosen to be a typical value for the given material and thickness. In the near threshold region the effect of any errors in the assumed value of A in the term K_{max}/A in the denominator will be small. As such the value of ΔK_{thr} is now chosen such that plot of the da/dN versus $\left[\frac{\Delta K - \Delta K_{thr}}{\sqrt{\{1 - K_{max}/A\}}}\right]$ data in the near threshold region, i.e. the low da/dN region, appears as a (near) straight line. The value of A is then fine tuned to improve linearity of the plot in the high ΔK region. This process is repeated for each of the R ratio data sets with the A value used being kept the same for each R ratio. This process will generally result in da/dN versus $\left[\frac{\Delta K - \Delta K_{thr}}{\sqrt{\{1 - K_{max}/A\}}}\right]$ plots that differ slightly in the high ΔK region. The value of A is then adjusted slightly, keeping the (adjusted) A the same for each R ratio, to minimise this difference, i.e. to better collapse the curves in the high ΔK region. This process will sometimes result in the various da/dN versus $\left[\frac{\Delta K - \Delta K_{thr}}{\sqrt{\{1 - K_{max}/A\}}}\right]$ curves associated with different R ratio's slightly diverging in the near threshold region. This is overcome by slightly tweaking the values of ΔK_{thr} until, allowing for experimental error, the various curve now essentially coincide. At this stage the values of ΔK_{thr}, for each R ratio, and the value of A have been obtained.

The values of D and m are then obtained directly from the Excel fit to the data.

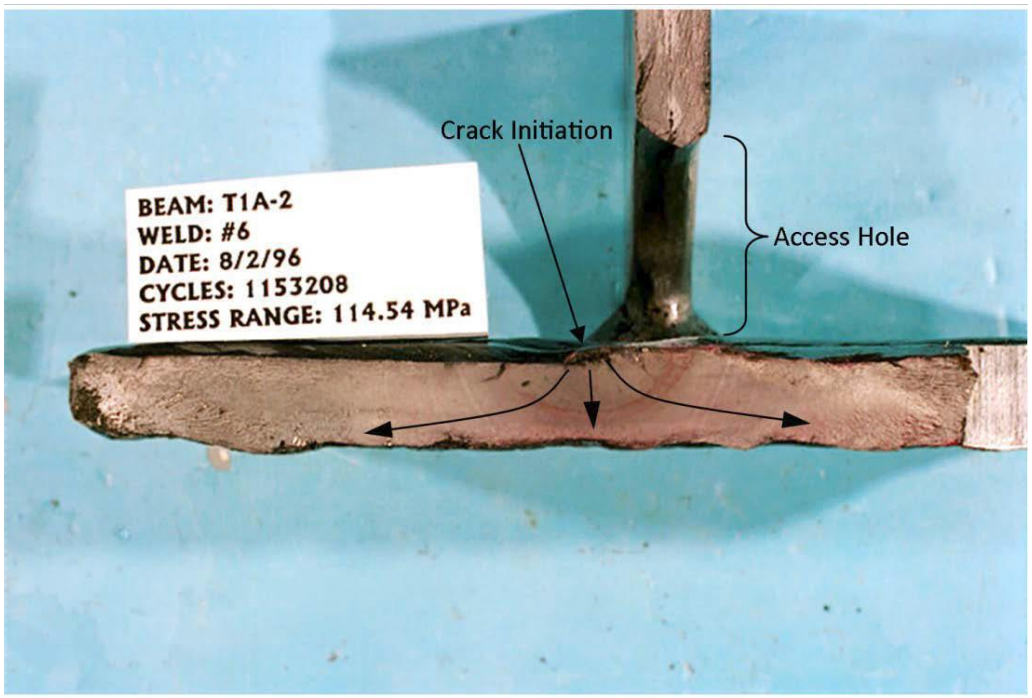

Figure 1 A typical bridge steel crack, from [17].

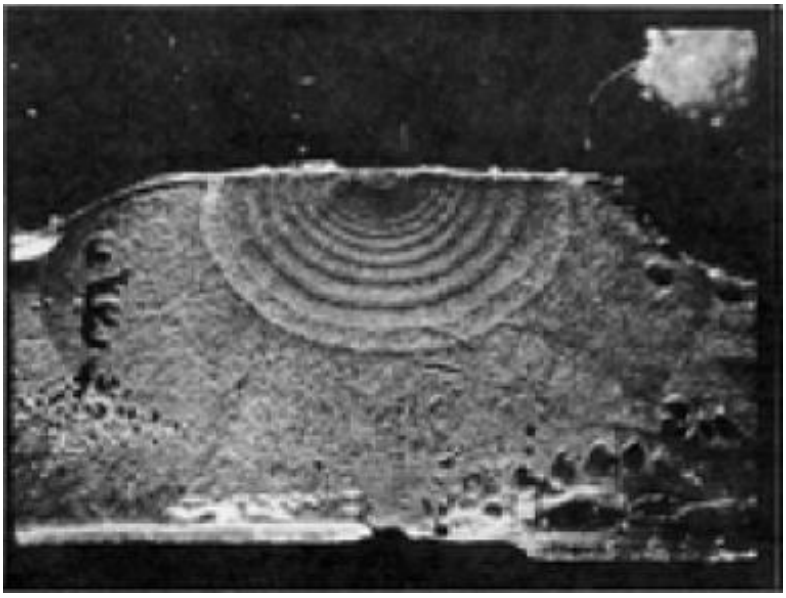

Figure 2 Cracking in the D6ac wing pivot fitting, from [27].

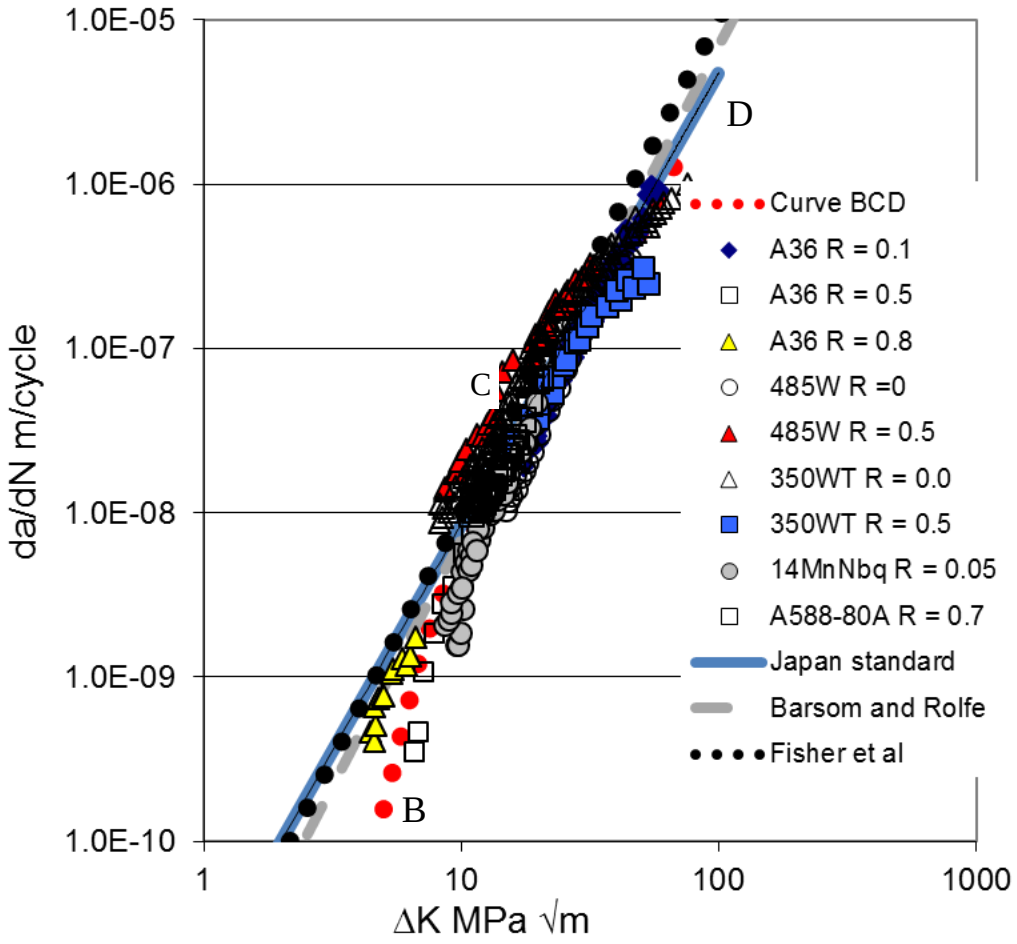

Figure 3 Representation of the growth of long cracks in a range of bridge steels and comparison with representations given in the literature.

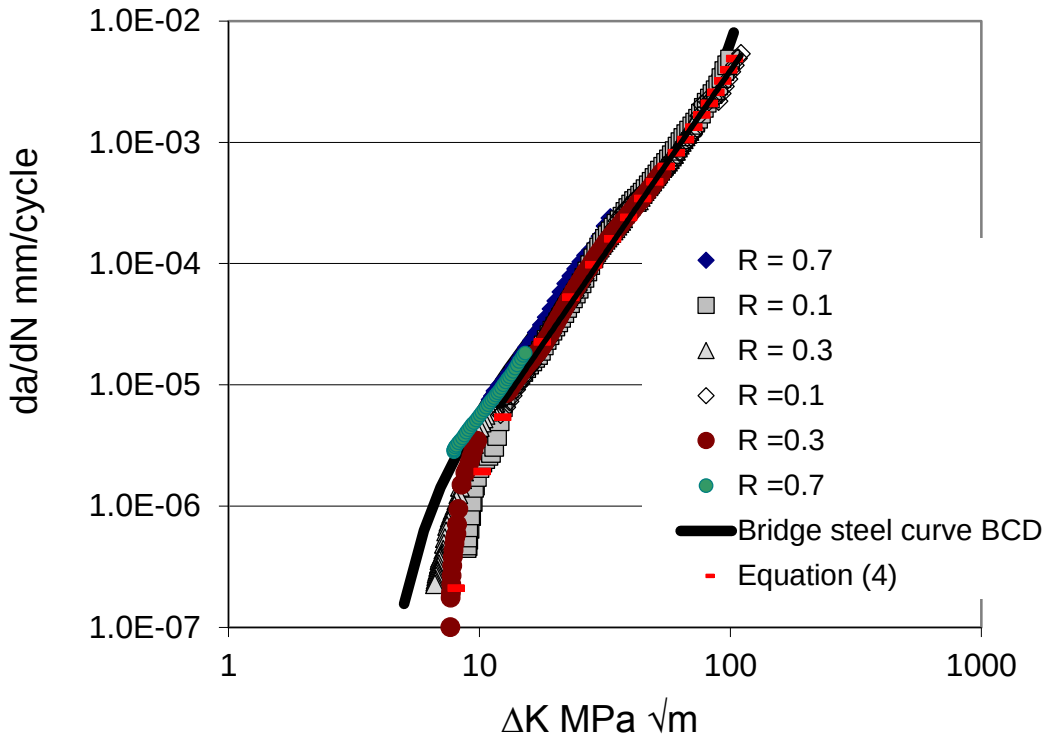

Figure 4 Comparison of the bridge steel curve BCD with the 4340 steel crack growth data taken from [20].

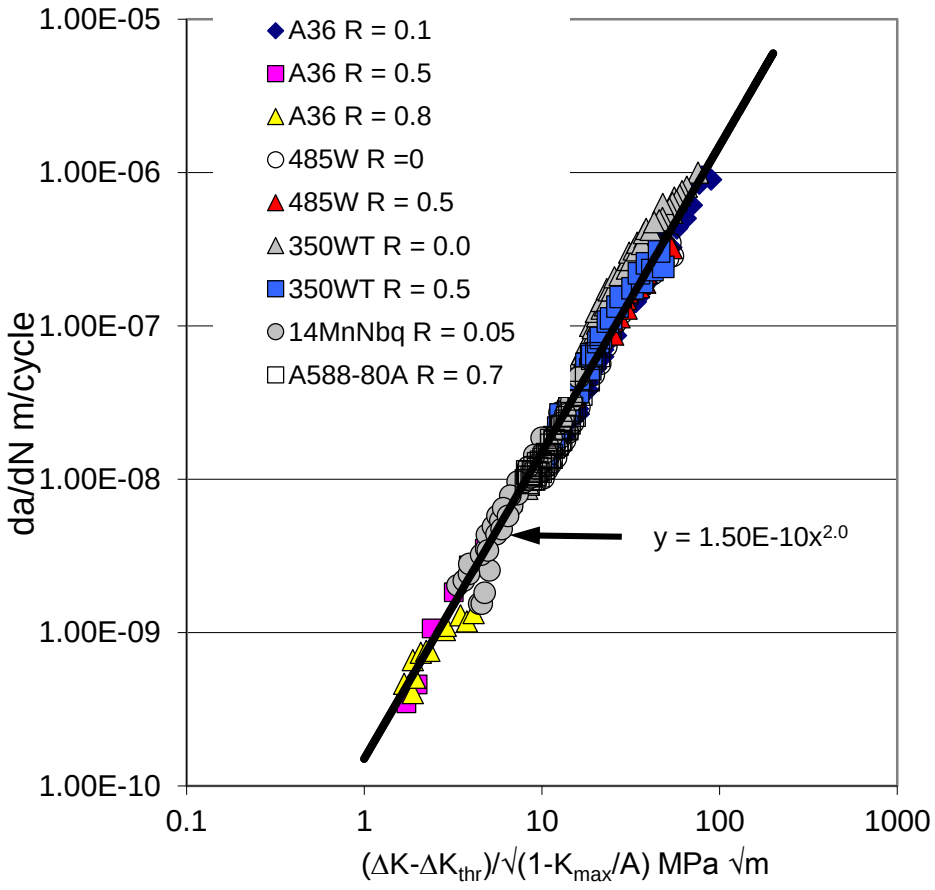

Figure 5 The NASGRO representation of crack growth in these bridge steels

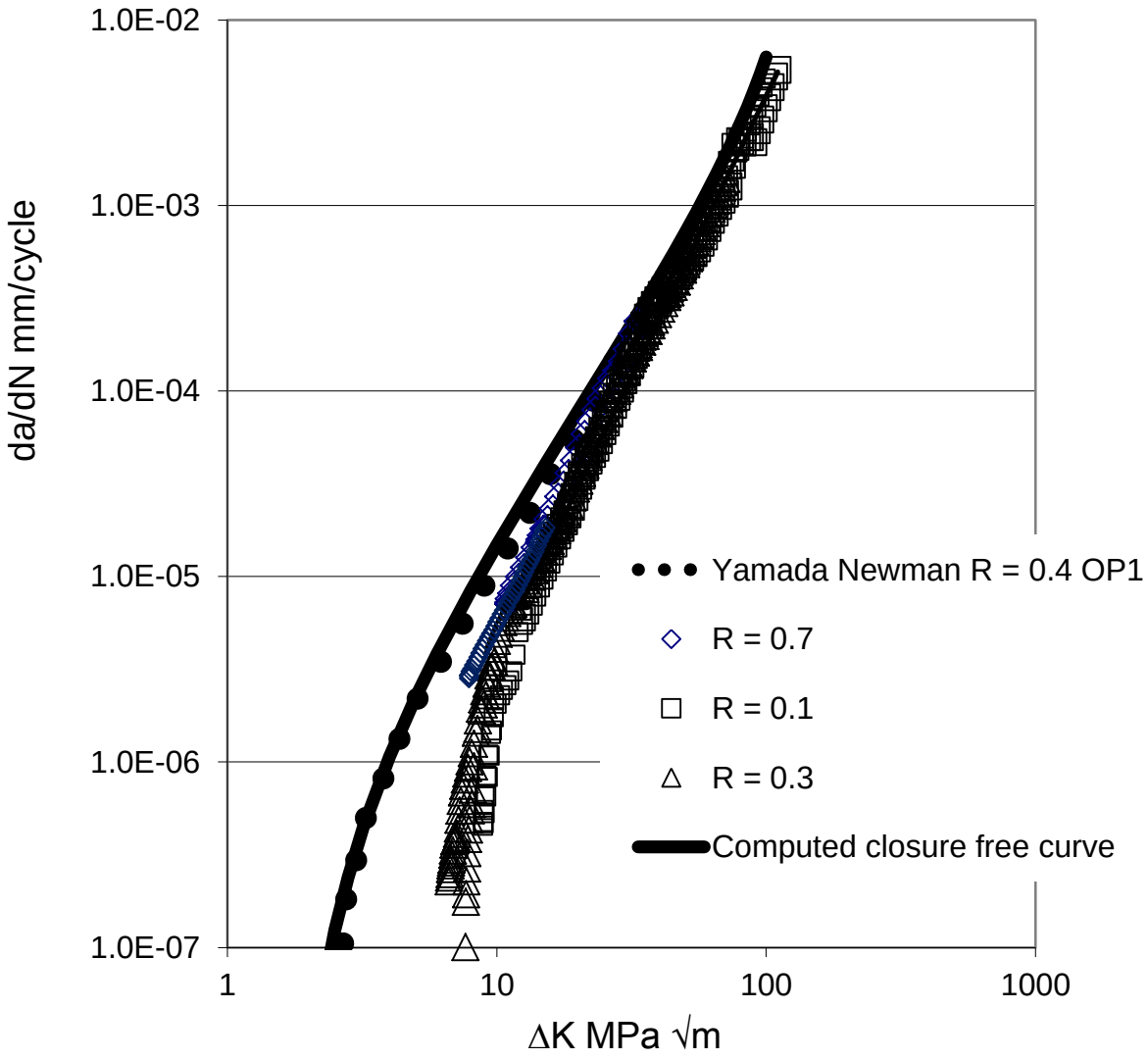

Figure 6 Measured and computed "closure free" curves for 4340 steel

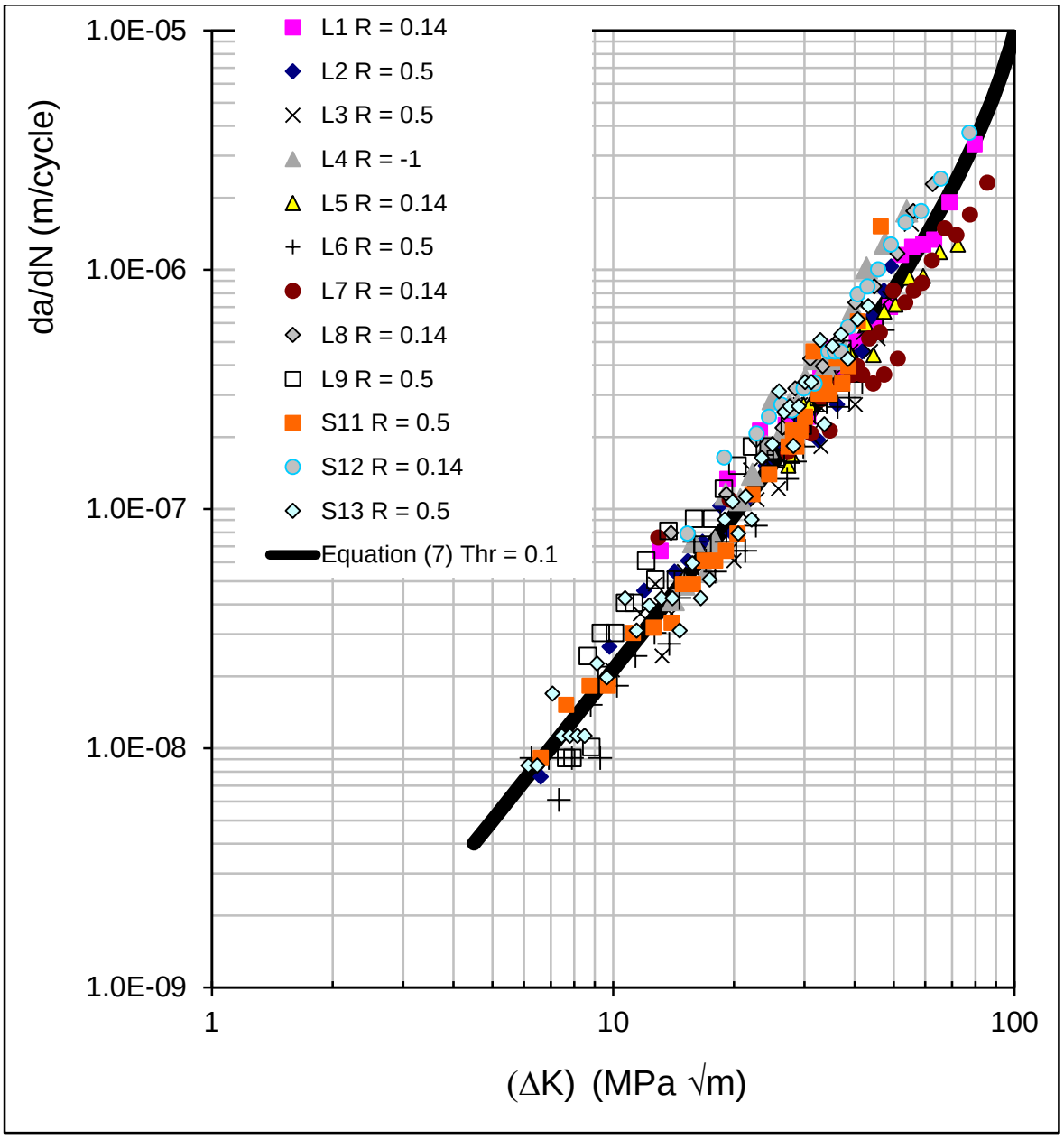

Figure 7 Crack growth da/dN versus ΔK curves associated with the small crack tests.

Figure 8 Corroded specimen prior to testing

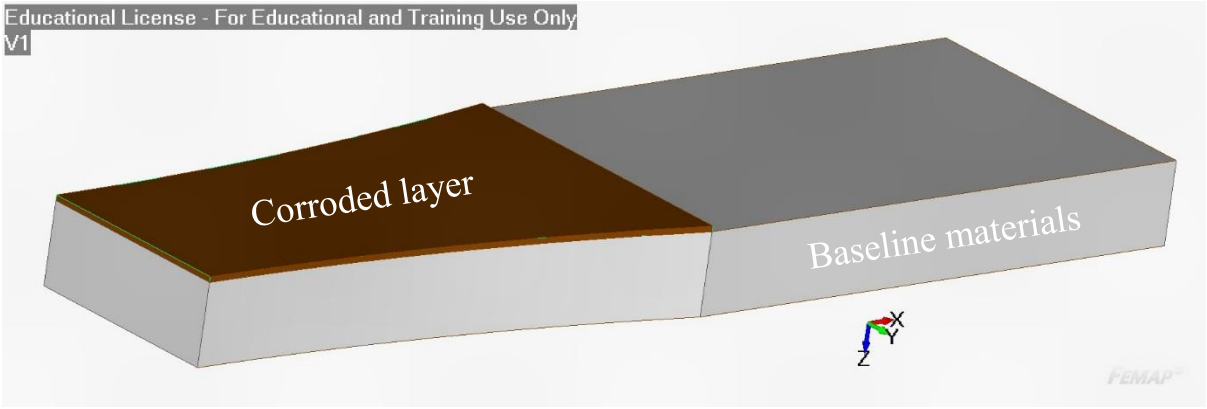

Figure 9 Half specimen is modelled.

Figure 10 View of the crossection

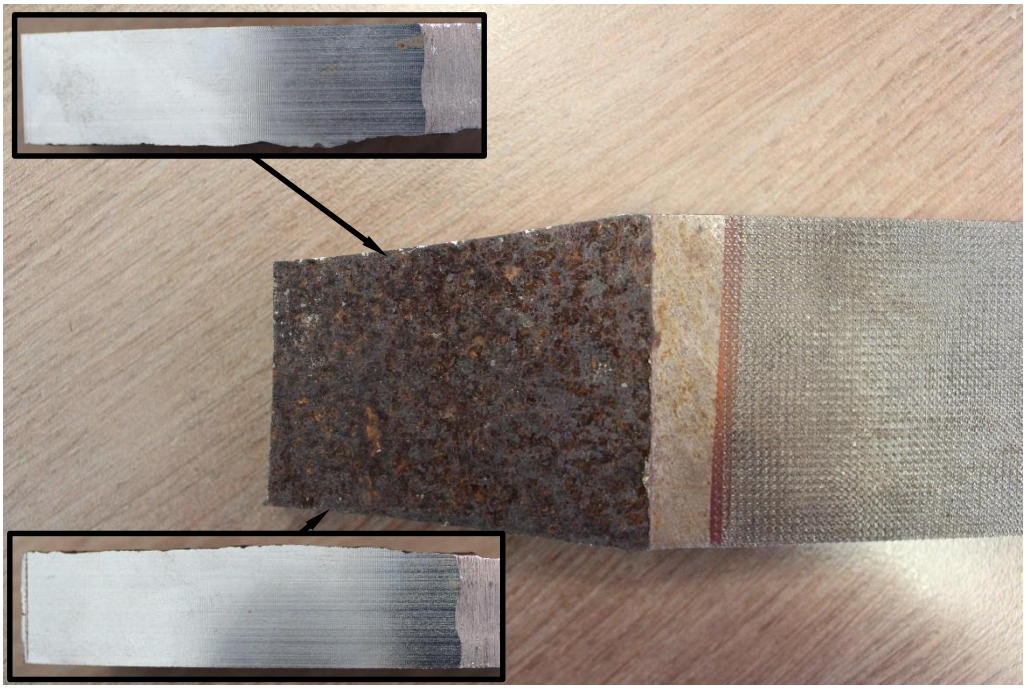

Figure 11 View of the crossection associated with the opposing part

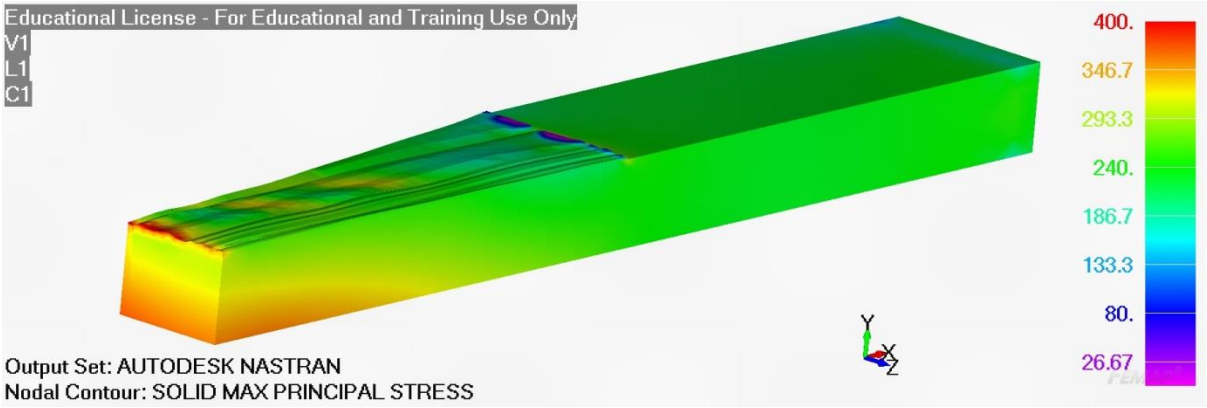

Figure 12 Effect of surface roughness

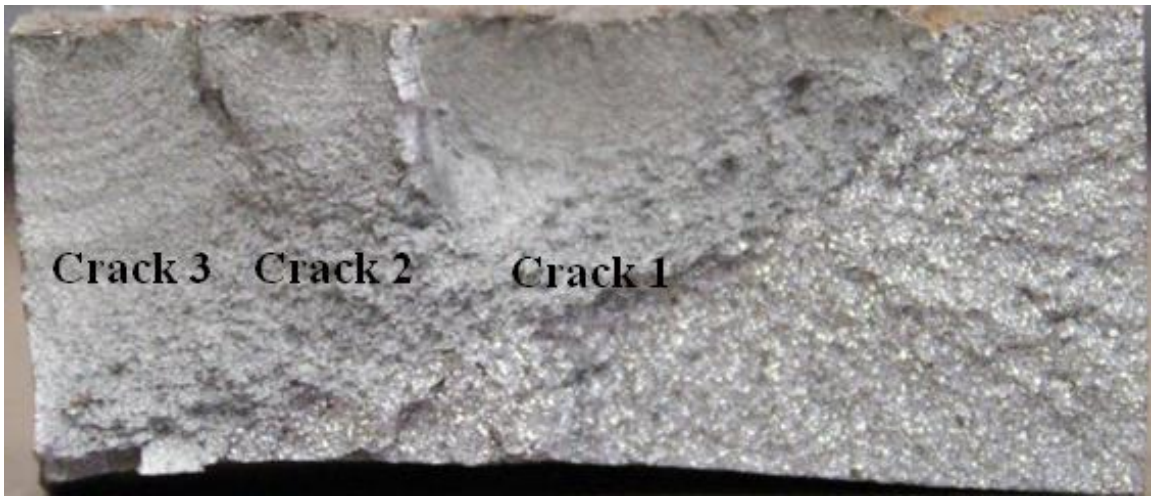

Figure 13 The three dominant cracks seen after failure of the specimen

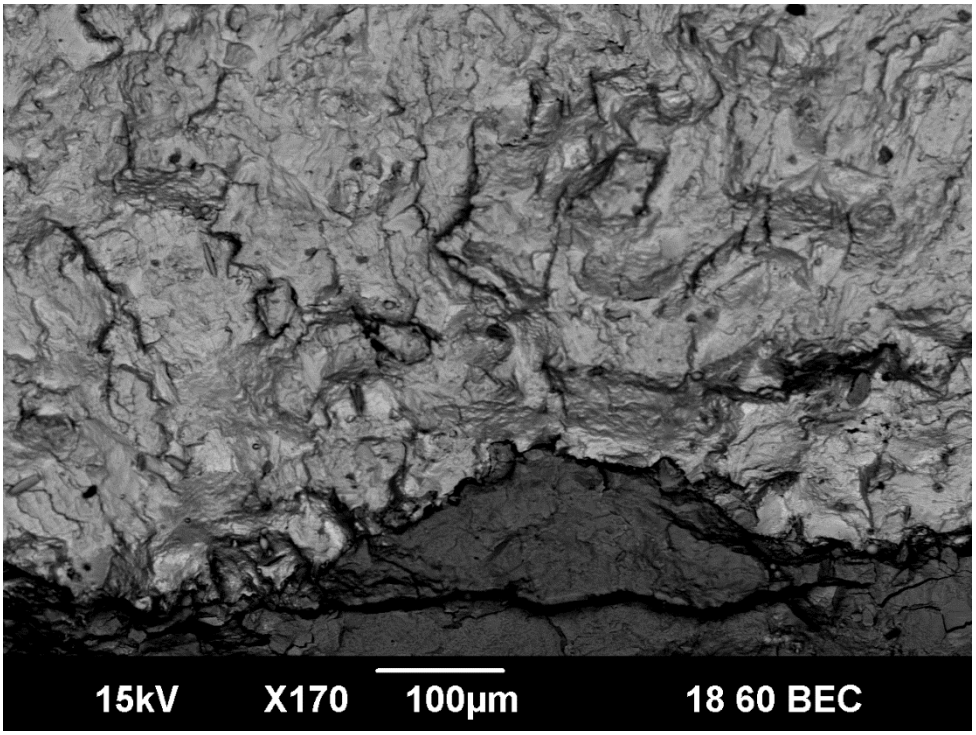

Figure 14 SEM of the initiating defect associated with crack 1.

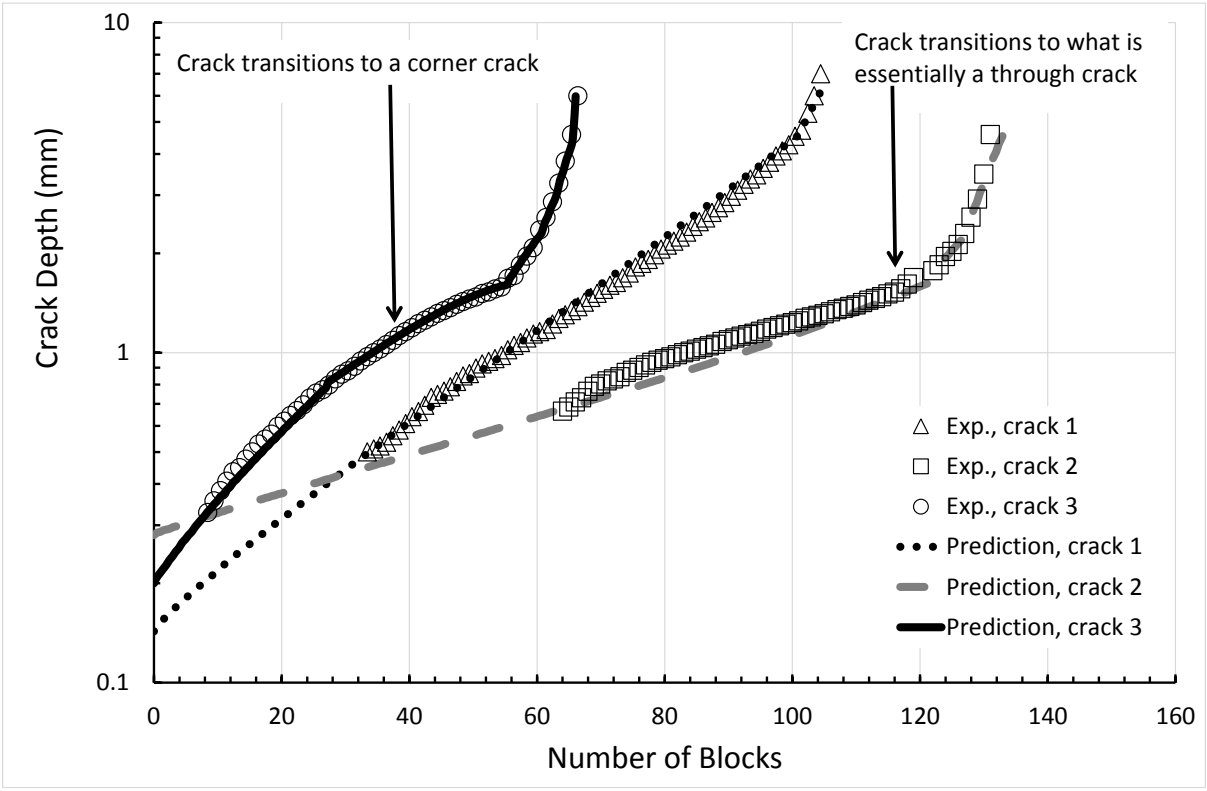

Figure 15 Comparison of measured and computed crack growth histories

Table 1 Values of ΔK (MPa √m) and da/dN associated with the curve BCD

ΔK (MPa √m)	da/dN (m/cycle)
5	1.56E-10
7	1.43E-09
8	2.56E-09
9	4.04E-09
10	5.87E-09
11	8.05E-09
13	1.35E-08
15	2.06E-08
20	4.56E-08
25	8.25E-08
30	1.33E-07
35	2.00E-07
40	2.85E-07
45	3.92 E-07
50	5.26 E-07
55	6.92 E-07
60	8.98 E-07
65	1.15 E-06
70	1.47 E-06
75	1.87E-06
80	2.37 E-06
85	3.02 E-06
90	3.88 E-06
95	5.05E-06
100	6.70E-06
105	9.18E-06

Table 2. Data and threshold values for the various tests

Materials	R ratio	ΔK_{thr} (MPa √m)	A (MPa √m)
A36	R ≈ 0.1	5.5	100
A36	R = 0.55	5	100
A36	R = 0.8	3	100
HPS 485 W	R = 0.0	5.5	120
HPS 485 W	R = 0.8	3.8	120
HPS 350 WT	R = 0.0	4.5	80
HPS 350 WT	R = 0.8	3	80
14MnNbq	R = 0.05	5.5	100
A588-80A	R = 0.7	3.2	90
A533 Grade B	R = 0.7	7.5	140
A533 Grade B, Class 1 weldment	R = 0.1	11	140

Table 3: Test envelope, from [40]

Specimen Number	D Width (mm)	Thickness (mm)	Notch (mm)	Area (mm^2)	R	σ_{max} (MPa)	σ_{min} (MPa)	$\Delta\sigma$ (MPa)	σ_{mean} (MPa)
L1	50.12	5.16	1.00	253.46	0.14	330.00	46.20	283.80	188.10
L2	50.15	5.41	1.00	265.90	0.50	330.00	165.00	165.00	247.50
L3	50.04	5.32	1.00	260.89	0.50	330.00	165.00	165.00	247.50
L4	49.94	5.38	1.00	263.30	-1.0	240.00	240.00	240.00	0.00
L5	50.00	5.64	1.00	276.36	0.14	330.00	46.20	283.80	188.10
L6	49.95	5.61	1.00	274.61	0.50	330.00	165.00	165.00	247.50
L7	49.95	5.64	1.00	276.08	0.14	330.00	46.20	283.80	188.10
L8	49.98	5.66	1.00	277.23	0.14	330.00	46.20	283.80	188.10
L9	50.11	5.65	1.00	277.47	0.50	330.00	165.00	165.00	247.50
S11	50.13	5.39	1.00	264.81	0.50	330.00	165.00	165.00	247.50
S12	50.11	5.64	1.00	276.98	0.14	330.00	46.20	283.80	188.10
S13	50.05	5.34	1.00	261.93	0.50	330.00	165.00	165.00	247.50

Table 4 Initial crack sizes

	Crack depth a mm	Half crack surface length c mm	ΔK_{thr} MPa $\sqrt{m}$
Crack 1	0.143	0.268	0.5
Crack 2	0.28	0.48	1.9
Crack 3	0.2	0.313	0.1